Supporting Information

Redox-Responsive, Reconfigurable All-Liquid Constructs

Huilou Sun, Mingwei Li, Lianshun Li, Tan Liu, Yuzheng Luo, Thomas P. Russell, and Shaowei Shi**

H. Sun, M. Li, L. Li, T. Liu, Y. Luo, Prof. S. Shi
Beijing Advanced Innovation Center for Soft Matter Science and Engineering, College of Materials Science and Engineering, Beijing University of Chemical Technology, Beijing 100029, China
E-mail: shisw@mail.buct.edu.cn
Prof. T. P. Russell
Department of Polymer Science and Engineering, University of Massachusetts, Amherst, Massachusetts 01003, USA
Materials Sciences Division, Lawrence Berkeley National Laboratory, 1 Cyclotron Road, Berkeley, California 94720, USA
E-mail: russell@mail.pse.umass.edu

Materials

$HAuCl_4$ (99%), sodium borohydride ($NaBH_4$, 98%), l-lactic acid (LLA, 98%), Poly-l-lactic acid (PLLA, M_n = 3.0 K), ferrocenemethanol (97%), tin 2-ethylhexanoate catalyst (96%), sodium hypochlorite (NaClO, 8% available chlorine), sodium dithionite ($Na_2S_2O_4$, 85%), and ferric chloride ($FeCl_3$, 98%) were purchased from J&K. Mono-6-thio-*β*-cyclodextrin (*β*-CD-SH, 98%) were purchased from Macklin. The above reagents were used as received unless otherwise noted. All anhydrous solvents (toluene (99.5%), dichloromethane (DCM, 99.5%), acetonitrile (MeCN, 99%), tetrahydrofuran (THF, 99%), carbon tetrachloride (CCl_4, 99.5%), N, N-dimethylformamide (DMF, 99.5%), n-hexane (97%), dimethyl sulfoxide (DMSO, 99.5%) and ethanol (99.7%)) were purchased from Sigma Aldrich and used without further purification.

Characterization

The apparent number-average molecular weights (M_n) and dispersities (M_w/M_n) were measured by size-exclusion chromatography (SEC), which was conducted with THF as the eluent. Polymerization was monitored by ^1H NMR spectroscopy using a Bruker Advance 400 MHz NMR spectrometer with $CDCl_3$ as solvent. Fourier transform infrared spectra (FTIR) was recorded on a Spectrum One spectrophotometer by 64 scans from 4000 to 500 cm^{-1} with a resolution of 4.0 cm^{-1}. The morphologies of emulsion and liquid tubule were characterized by polarized optical microscopy (ZEISS Imager.A2) or confocal fluorescence microscopy (Leica SP8). The size of *β*-CD NP was tested by DLS using Malvern Zetasizer Nano Series ZS90 and transmission electron microscopes (Hitachi HT 7700). The interfacial tension (γ) was analyzed by a multi-functional tensiometer (Krüss DSA30) using a pendent-drop method, where the evolution of γ with time was recorded after the water phase was slowly injected into the toluene phase. The deformation and wrinkle behavior were recorded as images or videos with a digital camera.

Redox Responsiveness

For the measurement of the interfacial tension and surface coverage in a redox process, the Fc-PLLA is firstly oxidized to Fc^+-PLLA by adding the oxidant (NaClO or $FeCl_3$) to Fc-PLLA toluene solution, then stirring at room temperature for 30 minutes. After filtering the precipitates, the obtained Fc^+-PLLA toluene solution is used for the pendent drop test by injecting *β*-CD NP aqueous solution into it. For the reduction process, the *β*-CD NP aqueous solution is added with the reductant ($Na_2S_2O_4$ or $NaBH_4$) firstly, then injected into the Fc^+-PLLA toluene solution. The Fc^+-PLLA is oxidized to Fc-PLLA at the interface, resulting the reinsertion of Fc into *β*-CD, as well as the formation and assembly of s-NPSs.

All-liquid 3D printing

A commercial JGAURORA 3D printer was modified to print aqueous tubules in toluene solution. The print head nozzle was replaced by a stainless steel syringe needle and connected with the syringe pump. The movement of the print head was controlled by Repetier-Host software. *β*-CD NP aqueous solution was injected into Fc-PLLA toluene solution at a flow rate of 0.7 mL min^{-1}. [*β*-CD NP] =20 mg mL^{-1}, [Fc-PLLA] =20 mg mL^{-1}. [1]

All-liquid molding

To construct structured liquids, for example, liquid letters, an aqueous *β*-CD NP solution was placed into the mold with a pattered trench, which had been prewetted with toluene solution of Fc-PLLA. After 10 minutes, the filled mold was immersed in an CCl_4 solution, producing liquids with desired shapes. [*β*-CD NP] =1.0 mg mL^{-1}, [Fc-PLLA] =1.0 mg mL^{-1}. [2]

Synthesis of *β*-cyclodextrin-modified gold nanoparticles (*β*-CD NP). The *β*-cyclodextrin-modified gold nanoparticles were synthesized according to the literature.[3-5] 200 mg $HAuCl_4$ was dissolved in 80 mL DMSO. 302 mg sodium borohydride ($NaBH_4$) and 44 mg mono-6-thio-*β*-cyclodextrin (*β*-CD-SH) were dissolved in 80 mL DMSO. The reaction mixture turned deep brown immediately when two kinds of solutions were mixed. After reacting for 24 h, the particles were precipitated by adding 160 mL acetonitrile and then collected by centrifugation. After washing the precipitate with 120 mL acetonitrile: DMSO (1:1 v/v) and 120 mL ethanol, *β*-CD NPs were isolated by centrifugation, and freeze-dried under vacuum for 24 h. The FT-IR spectrum can prove that *β*-cyclodextrin is successfully anchored to gold nanoparticles (Figure S1). The size of the synthesized nanoparticles is around 5.0 nm from TEM (Figure S2). The average number of *β*-CD molecules anchored to each gold NP can be calculated using the surface areas of *β*-CD and gold NP. The surface area of *β*-CD is ~180 $Å^2$. The surface area of gold NP (5 nm) is ~7400 $Å^2$ and the surface coverage is estimated to be ~80%.

Therefore, on average, there are ~33 *β*-CD molecules anchored to each gold NP. FT-IR (KBr, cm^{-1}): *v* = 1033 (V_{C-O} in *β*-CD), 1405 (V_{C-C} in *β*-CD), 2929 (V_{-CH3} and V_{-CH2} in *β*-CD), 3426 (V_{O-H} in *β*-CD).

Synthesis of Ferrocene-terminated Poly-l-lactic acid (Fc-PLLA).[5, 6] 2.9 g l-lactic acid (LLA) and 0.2 g ferrocenemethanol were added into a 25 mL Schlenk flask. Three freeze-pump-thaw cycles were performed to remove the oxygen. The flask was immersed into an oil bath at 115 ℃ with vigorous magnetic stirring for 5.0 min. Then 4.0 mg tin 2-ethylhexanoate catalyst in dry 1.0 mL DMF was added to the mixture via a microsyringe. After reacting for 2.0 h at 115 ℃, the crude product was dissolved in hot CH_2Cl_2, and the solution was precipitated into *n*-hexane. The product was washed by three times. The final product was dried in vacuum, yielding a light yellow solid (2.6 g, 83%). FT-IR (KBr, cm^{-1}): *v* = 694, 765 (V_{C-H} in Fc), 1457 ($V_{C=O}$ in PLLA), 2948 (V_{C-H} in PLLA), 2999 (V_{C-H} in PLLA). ^{1}H NMR (400 MHz, $CDCl_3$, δ): 5.2 (s, 2H), 1.84-1.14 (m, 6H). M_n = 3000, M_w = 3400, PDI = 1.1.

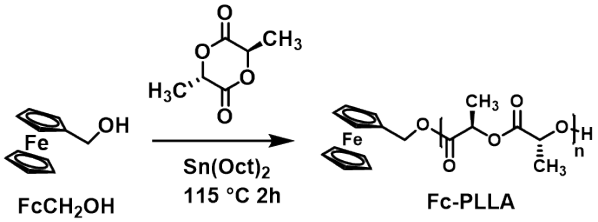

Scheme S1. Synthetic route of Fc-PLLA.

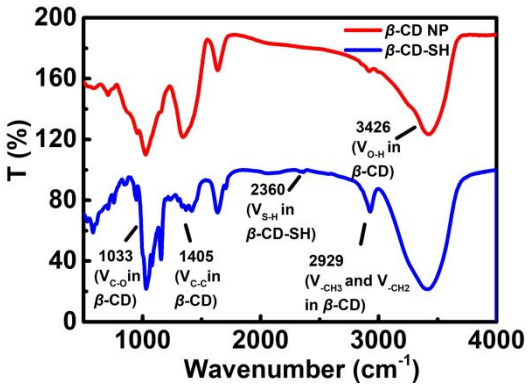

Figure S1. FT-IR spectra of *β*-CD-SH and *β*-CD NP.

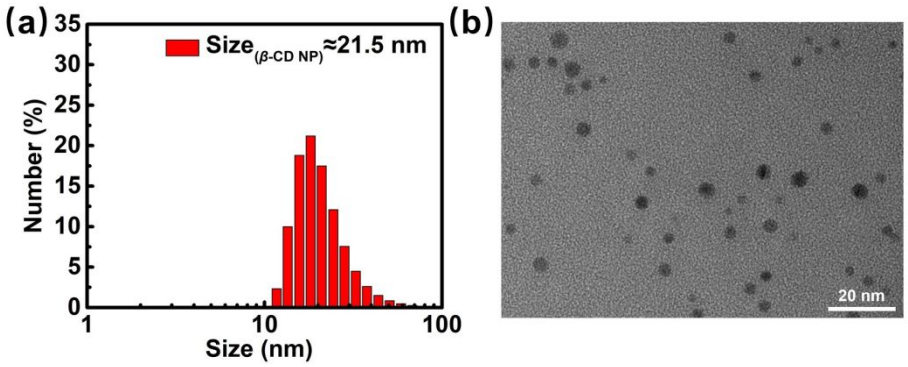

Figure S2. (a) DLS and (b) TEM image of *β*-CD NP.

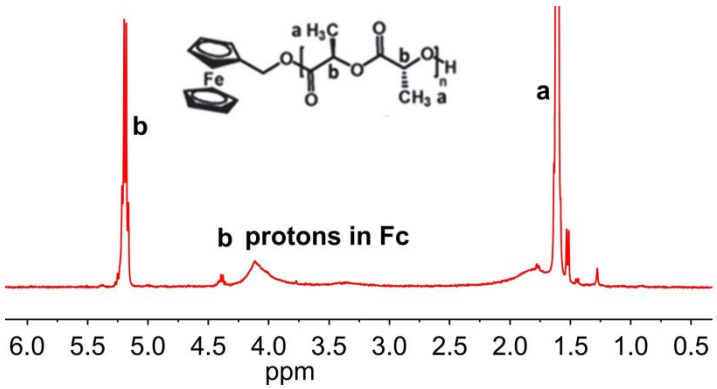

Figure S3. ^{1}H-NMR spectrum of Fc-PLLA in $CDCl_3$.

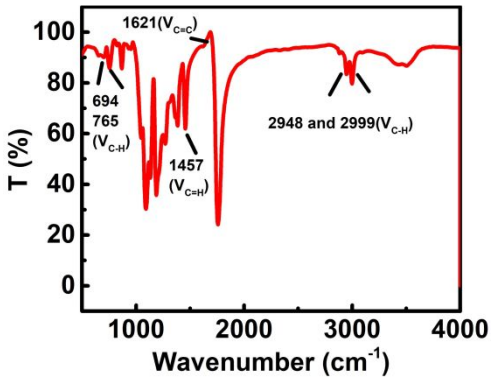

Figure S4. FT-IR spectrum of Fc-PLLA.

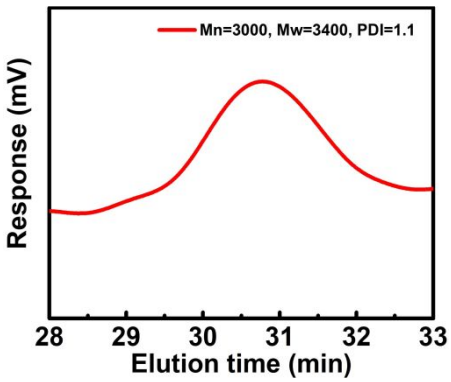

Figure S5. SEC spectrum of Fc-PLLA.

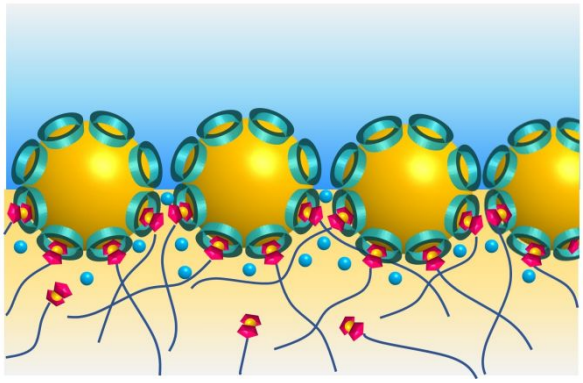

Figure S6. Schematic of the high energy toluene environment with water molecules.

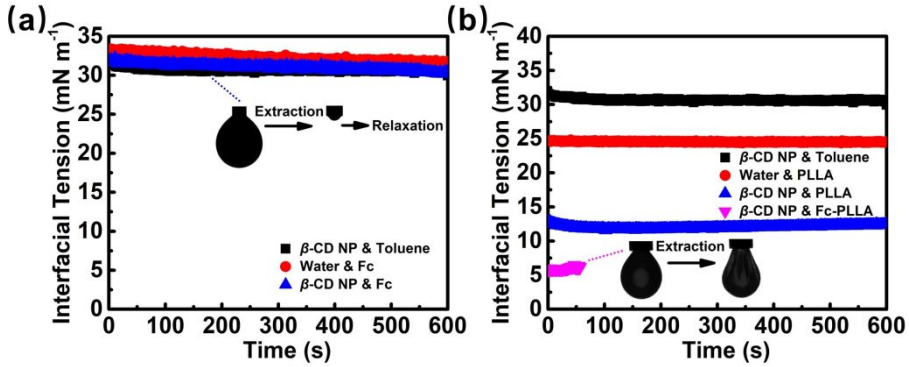

Figure S7. (a) Time evolution of interfacial tension of different oil-water systems including *β*-CD NP@water/toluene, water/Fc@toluene and *β*-CD NP@water/Fc@toluene; (b) time evolution of interfacial tension of different oil-water systems including *β*-CD NP@water/toluene, water/ PLLA@toluene, *β*-CD NP@water/ PLLA@toluene and *β*-CD NP@water/ Fc-PLLA@toluene. [*β*-CD NP] = 1.0 mg mL^{-1}, [Fc] = 1.0 mg mL^{-1}, [PLLA] = 1.0 mg mL^{-1}, [Fc-PLLA] = 1.0 mg mL^{-1}.

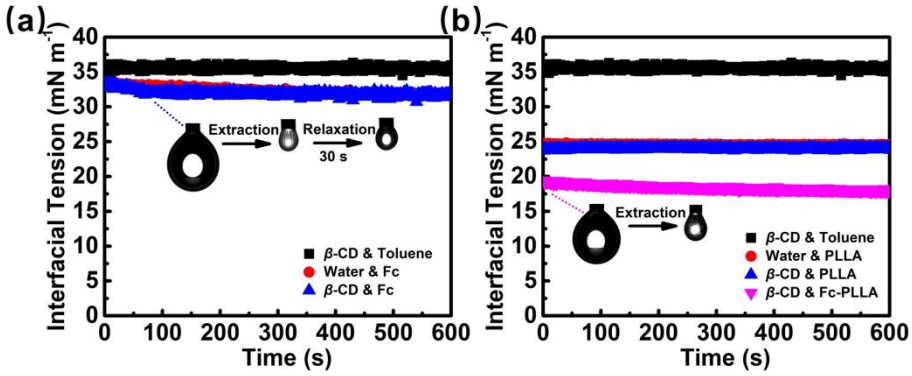

Figure S8. (a) Time evolution of interfacial tension of different oil-water systems including *β*-CD@water/toluene, water/Fc@toluene and *β*-CD@water/Fc@toluene; (b) time evolution of interfacial tension of different oil-water systems including *β*-CD @water/toluene, water/ PLLA@toluene, *β*-CD@water/ PLLA@toluene and *β*-CD @water/ Fc-PLLA@toluene. [*β*-CD] = 1.0 mg mL^{-1}, [Fc] = 1.0 mg mL^{-1}, [PLLA] = 1.0 mg mL^{-1}, [Fc-PLLA] = 1.0 mg mL^{-1}.

For the systematic study of the interactions at the interface, we first discuss the interactions between *β*-CD NPs and Fc molecules at the water-toluene interface (Figure S7a). As discussed in the manuscript, due to the amphiphilicity of *β*-CD, *β*-CD NPs show a weak interfacial activity at the toluene-water interface (~30 mN m^{-1}). Toluene could interact with *β*-CD to form inclusion complexes (the association constant of toluene for *β*-CD is ~1.4×10^2 M^{-1}). [7] However, due to the full inclusion of toluene in the cavity of *β*-CD, it will not result in a large change in the interfacial activity of *β*-CD NPs. With 1.0 mg mL^{-1} Fc dissolved in toluene against pure water, the interfacial tension is ~33 mN m^{-1}, which is slightly lower than that of the pure water-toluene system (~36 mN m^{-1}) since a small quantity of Fc is oxidized to Fc^+ in storage and adsorbed to the negatively charged oil-water interface. When contracting the droplet, no wrinkles are observed, indicating the binding energy of either *β*-CD NPs or Fc (Fc^+) is too low to support a load. With 1.0 mg mL^{-1} *β*-CD NPs dissolved in water against 1.0 mg mL^{-1} Fc dissolved in toluene, the interfacial tension is ~30 mN m^{-1}, which is almost the same with that of *β*-CD NPs, indicating the interfacial activity of *β*-CD NPs is not changed.

Interestingly, when contracting the droplet, wrinkling is observed at large volume reductions, but the wrinkles relax rapidly, indicating that the binding energy of *β*-CD NPs at the interface is slightly enhanced. The only reasonable explanation is the formation of *β*-CD/Fc inclusion complexes at the interface (although Fc can also be included in *β*-CD, the bigger size of Fc than toluene will slightly enhance the amphiphilicity of inclusion complexes; the association constant of Fc for *β*-CD is ~1.7×10^4 M^{-1}). [8] Even without PLLA, there is a small amounts of water in the toluene close to the interface, triggering the host-guest interactions. However, due to the hydrophobic nature of Fc, only a few Fc can move to the interface to interact with β-CD, which is a random collision process. Thus, it does not result in a large change in the interfacial activity of *β*-CD NPs.

To stress the importance of PLLA in our system, the interactions between pure PLLA and *β*-CD NPs were also investigated. As shown in Figure S7b, with 1.0 mg mL^{-1} pure PLLA dissolved in toluene against water, an obvious reduction in the interfacial tension from ~36 to ~24 mN m^{-1} is observed, indicating the surfactant nature of PLLA, due to the hydrogen bonding between PLLA carbonyl groups and water. With 1.0 mg mL^{-1} *β*-CD NPs dissolved in water against 1.0 mg mL^{-1} PLLA dissolved in toluene, the interfacial tension decreases to ~12 mN m^{-1}, due to the formation of hydrogen bonds between PLLA and hydroxyl groups of *β*-CD NPs at the interface. However, when the droplet is compressed, no wrinkling is seen, indicating that the binding energy of *β*-CD NPs is too low to support a load at the interface, even with the hydrogen bonding. On the other hand, as we have shown in the manuscript, with 1.0 mg mL^{-1} *β*-CD NPs dissolved in water against 1.0 mg mL^{-1} Fc-PLLA dissolved in toluene, the interfacial tension rapidly decreases to ~6.0 mN m^{-1}, and the interface rapidly saturates. No relaxation of wrinkles is observed when contracting the droplet. These results give a strong evidence that, in addition to the hydrogen bonding, host-guest interactions occur at the interface, greatly enhancing the binding energy of *β*-CD NPs. As mentioned in the manuscript, with hydrogen bonding, the terminal Fc groups and *β*-CD NPs can locate at the

toluene−water interface, significantly enhancing the probability of collision, leading to rapid triggering of molecular recognition in a high energy toluene environment with water molecules.

We also studied the *β*-CD/Fc, *β*-CD/PLLA and *β*-CD/Fc-PLLA interactions at the toluene-water interface (Figure S8). The results are similar to those of the *β*-CD NP-based systems (Figure S7). It should be noted that in Figure S8b, with *β*-CD dissolved in the water and pure PLLA dissolved in the toluene, the equilibrium interfacial tension is almost the same as that only the pure PLLA dissolved in the toluene, indicating the decreased interfacial tension mainly arises from the PLLA, since, in comparison to *β*-CD NPs, the size of *β*-CD is much smaller, and the reduction in the interfacial energy for each *β*-CD is very low. Thus *β*-CD easily desorbs from the interface even with hydrogen bonding between the hydroxyl groups of *β*-CD and carbonyl groups of PLLA.

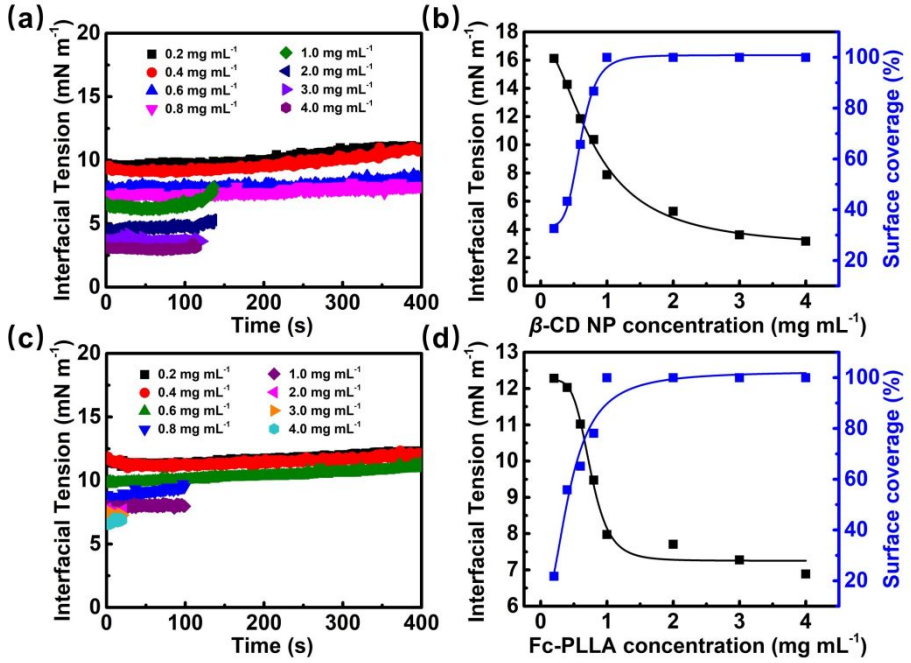

Figure S9. (a) Time evolution of interfacial tension with different concentrations of *β*-CD NP from 0.2 to 4.0 mg mL^{-1}, [Fc-PLLA] = 0.5 mg mL^{-1}; (b) equilibrium interfacial tension and surface coverage as a function of *β*-CD NP concentration; (c) time evolution of interfacial tension with different concentrations of Fc-PLLA from 0.2 to 4.0 mg mL^{-1}, [*β*-CD NP] = 0.5

mg mL^{-1}; (d) equilibrium interfacial tension and surface coverage as a function of Fc-PLLA concentration.

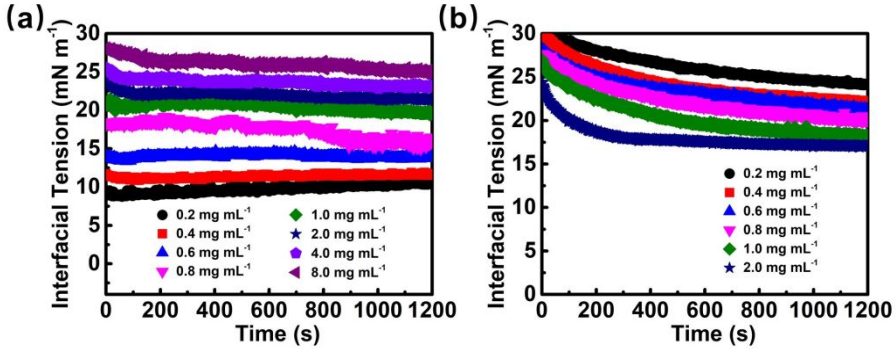

Figure S10. (a) Time evolution of interfacial tension by varying the concentration of NaClO in the oil phase; (b) time evolution of interfacial tension by varying the concentration of $Na_2S_2O_4$ in the water phase. [β-CD NP]=1.0 mg mL^{-1}, [Fc-PLLA]=1.0 mg mL^{-1}.

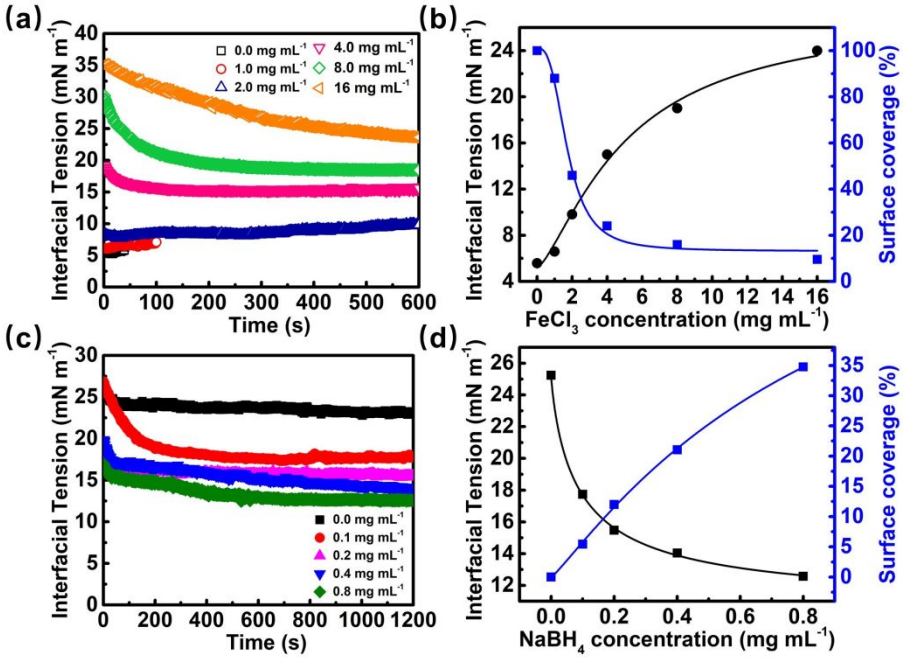

Figure S11. (a) Time evolution of interfacial tension by varying the concentration of $FeCl_3$ in the oil phase; (b) interfacial tension and surface coverage as a function of $FeCl_3$ concentration; (c) time evolution of interfacial tension by varying the concentration of $NaBH_4$ in the water phase; (d) interfacial tension and surface coverage as a function of $NaBH_4$ concentration. [β-CD NP]=1.0 mg mL^{-1}, [Fc-PLLA]=1.0 mg mL^{-1}.

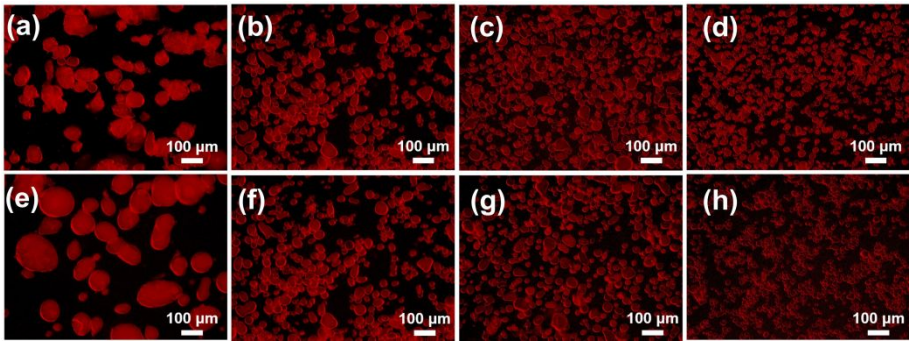

Figure S12. Fluorescence microscopy images of structured emulsions at different *β*-CD NP concentrations of (a) 0.5 mg mL^{-1}, (b) 1.0 mg mL^{-1}, (c) 2.0 mg mL^{-1}, and (d) 4.0 mg mL^{-1}, [Fc-PLLA]=1.0 mg mL^{-1}; fluorescence microscopy images of emulsions droplets at different Fc-PLLA concentrations of (e) 0.5 mg mL^{-1}, (f) 1.0 mg mL^{-1}, (g) 2.0 mg mL^{-1}, and (h) 4.0 mg mL^{-1}, [*β*-CD NP] = 1.0 mg mL^{-1}. [Rhodamine B] = 0.5 mg mL^{-1}, w/o = 1:6; shear rate = 15000 rpm; shear time = 3.0 min.

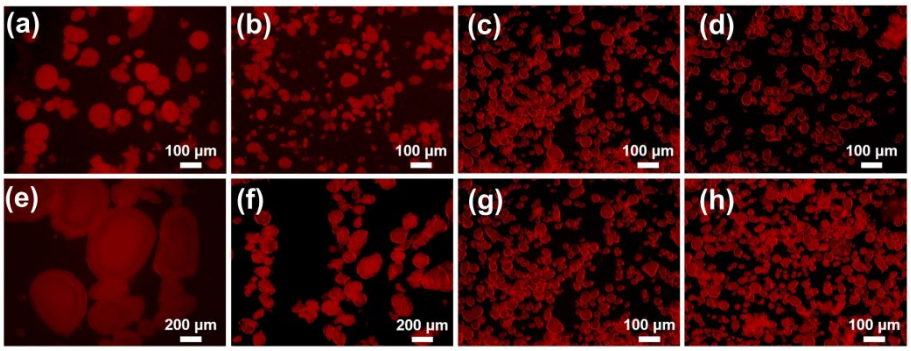

Figure S13. (a) Fluorescence microscopy images of emulsion droplets at different shear rate of (a) 5000 rpm, (b) 10000 rpm, (c) 15000 rpm and (d) 35000 rpm, shear time = 3.0 min; fluorescence microscopy images of emulsion droplets at different shear time of (e) 0.5 min, (f) 1.0 min, (g) 3.0 min and (h) 6.0 min, shear rate = 15000 rpm. [*β*-CD NP] = 1.0 mg mL^{-1}, [Fc-PLLA] = 1.0 mg mL^{-1}, [Rhodamine B] = 0.5 mg mL^{-1}, w/o = 1:6.

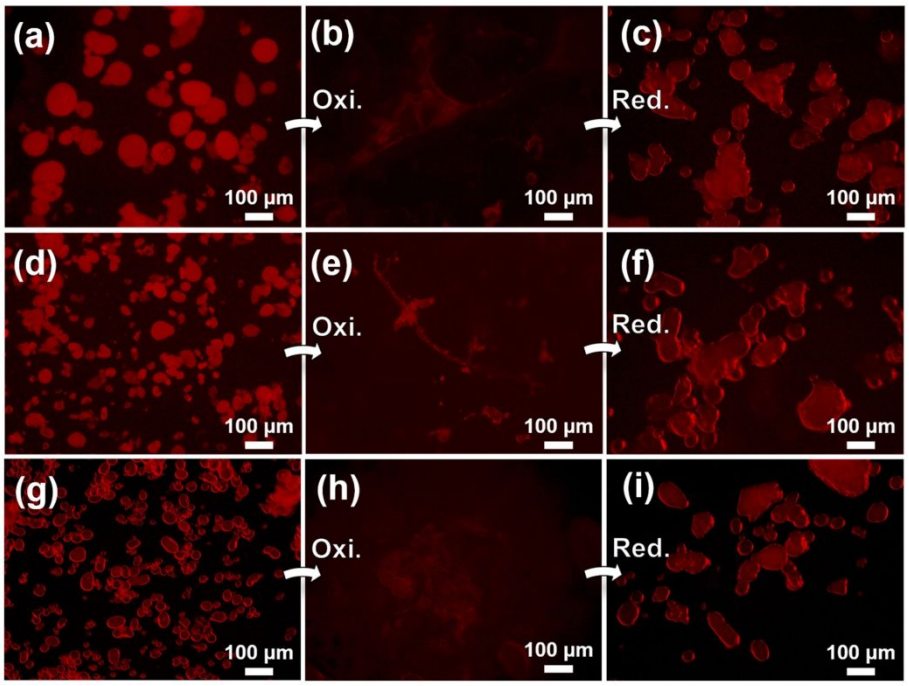

Figure S14. (a) Fluorescence microscopy images of emulsification/demulsification process of emulsion droplets prepared at different shear rate of (a) 5000 rpm, (d) 10000 rpm, (g) 35000 rpm, shear time = 3.0 min. [β-CD NP] = 1.0 mg mL^{-1}, [Fc-PLLA] = 1.0 mg mL^{-1}, [NaClO] = 4.0 mg mL^{-1}, [$Na_2S_2O_4$] = 2.0 mg mL^{-1}, [Rhodamine B] = 0.5 mg mL^{-1}, w/o = 1:6.

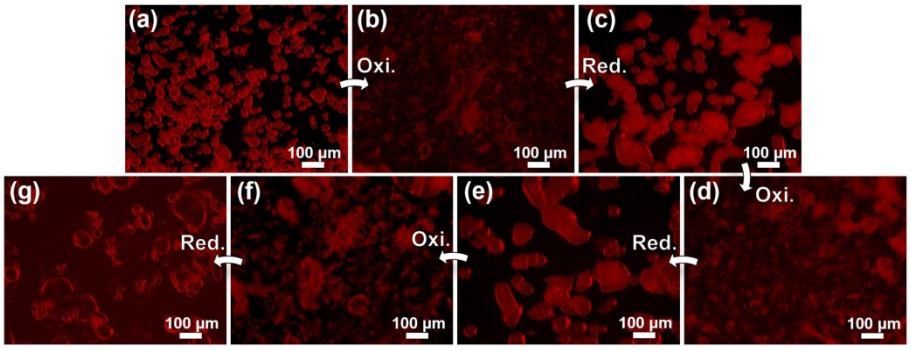

Figure S15. Fluorescence microscopy images showing the repeatedly switchable emulsification/demulsification process for three times. [β-CD NP] = 1.0 mg mL^{-1}, [Fc-PLLA] = 1.0 mg mL^{-1}, [NaClO] = 4.0 mg mL^{-1}, [$Na_2S_2O_4$] = 2.0 mg mL^{-1}, [Rhodamine B] = 0.5 mg mL^{-1}.

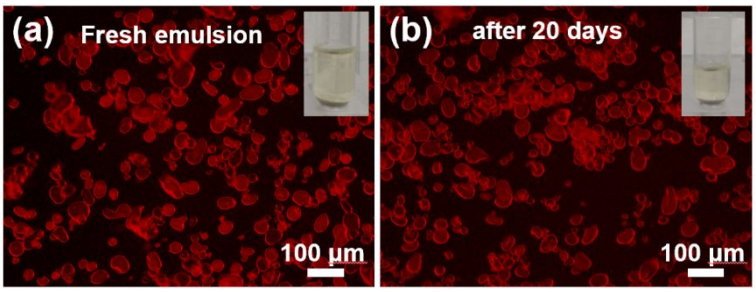

Figure S16. Fluorescence microscopy images of showing the irregular shapes of the emulsions retains after 20 days. [β-CD NP] = 1.0 mg mL^{-1}, [Fc-PLLA] = 1.0 mg mL^{-1}, [Rhodamine B] = 0.5 mg mL^{-1}.

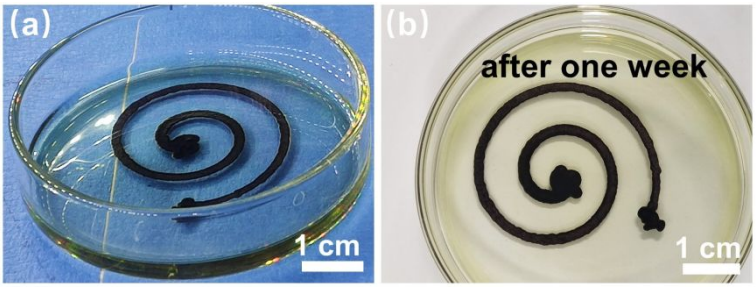

Figure S17. (a) Optical image of the just prepared liquid device using all-liquid 3D printing; (b) optical image of liquid device one week after preparation. [β-CD NP] = 20 mg mL^{-1}, [Fc-PLLA] = 20 mg mL^{-1}.

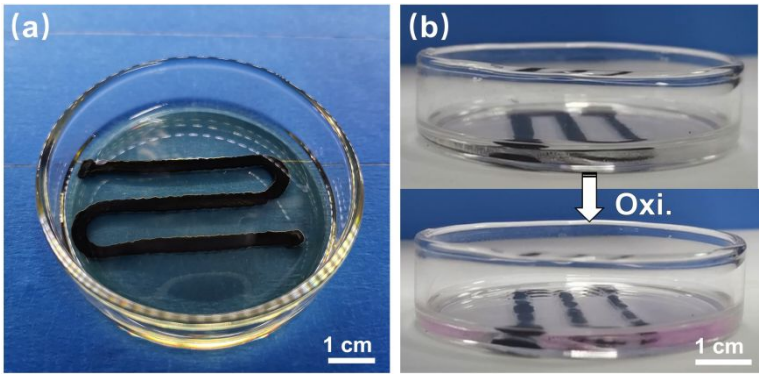

Figure S18. (a) Optical image of the prepared liquid device using all-liquid 3D printing; (b) optical iamge of liquid device showing the release of Rhodamine B with the addition of NaClO solution into the toluene phase near the tubules. [β-CD NP] = 20 mg mL^{-1}, [Fc-PLLA] = 20 mg mL^{-1}, [Rhodamine B] = 0.5 mg mL^{-1}, [NaClO] = 100 mg mL^{-1}.

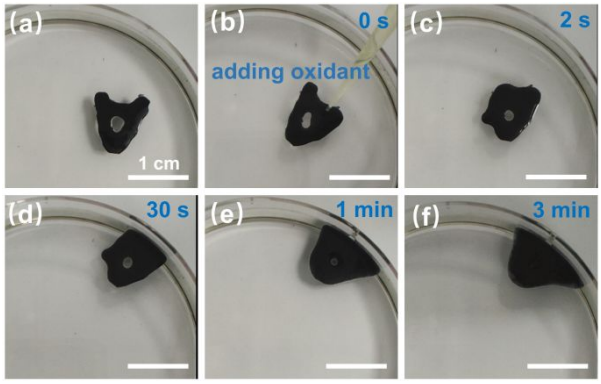

Figure S19. Optical images of liquid letter "A" prepared using all-liquid molding showing the collapse of the liquid structure with the addition of 200 μL NaClO onto the surface of liquid letter. [β-CD NP] = 1.0 mg mL^{-1}, [Fc-PLLA] = 1.0 mg mL^{-1}, [NaClO] = 100 mg mL^{-1}.

References

[1] J. Forth, X. Liu, J. Hasnain, A. Toor, K. Miszta, S. Shi, P. L. Geissler, T. Emrick, B. A. Helms, T. P. Russell, *Adv. Mater.* **2018**, *30*, 1707603.

[2] S. Shi, X. Liu, Y. Li, X. Wu, D. Wang, J. Forth, T. P. Russell, *Adv. Mater.* **2018**, *30*, 1705800.

[3] (a) Rojas, M. T.; Königer, R.; Stoddart, J. F.; Kaifer, A. E., *J. Am. Chem. Soc.* **1995**, *117*, 336; (b) J. Liu, J. Alvarez, W. Ong, E. Rom n, A. E. Kaifer, *J. Am. Chem. Soc.* **2001**, *123*, 11148.

[4] L. Peng, M. You, C. Wu, D. Han, I. Csoy, T. Chen, Z. Chen and W. Tan, *ACS Nano* **2014**, *8*, 2555.

[5] H. Sun, L. Li, T. P. Russell, S. Shi, *J. Am. Chem. Soc.* **2020**, *142*, 8591.

[6] Y. Xia, B. D. Olsen, J. A. Kornfield, R. H. Grubbs, *J. Am. Chem. Soc.* **2009**, *131*, 18525.

[7] I. Sanemasa, Y. Akamine, *Bull. Chem. Soc. Jpn.* **1987**, *60*, 2059.

[8] J.- S. Wu, K. Toda, A. Tanaka, I. Sanemasa, *Bull. Chem. Soc. Jpn.* **1998**, *71*, 1615.